



OPEN Early warnings are too late when parameters change rapidly

Rohit Radhakrishnan^{1,2}, Induja Pavithran^{1,2,6}, Valerie Livina³, Jürgen Kurths^{4,5}✉ & R. I. Sujith^{1,2}✉

Tipping (or sudden transition) from a desirable state to an undesirable one can result in catastrophic changes, affecting natural environments, human societies and economies. Early warning signals (EWSs) are developed to forewarn such an impending tipping. However, when control parameters are varied fast, we observe that EWSs detect an impending tipping past bifurcation points; this questions the applicability of EWSs in preventing tipping. At the same time, the fast rate of change of parameter delays the actual tipping event, providing a borrowed window of safe operation. This delay in tipping offers a window for prevention through swift action. We demonstrate instances of both successful and unsuccessful preventions, in a paradigmatic thermoacoustic system—a horizontal Rijke tube. This work highlights the interplay of warning time, choice of prevention action and rate of variation of parameters in EWS-based prevention of tipping.

Tipping point refers to a critical moment or a threshold of control parameter beyond which a system undergoes a sudden and often irreversible change in its behavior^{1–3}. Such a sudden transition from a desirable state to an undesirable one can result in catastrophic changes, affecting natural environments, human societies and economies. Several generic early warning signals (EWSs) are developed to forewarn such an impending tipping^{4–8}.

The primary focus of the research on EWSs involves the identification of indicators across various systems to predict tipping⁹. In the case of bifurcation induced tipping, the responses to perturbations slow down on approaching a bifurcation point, a phenomenon known as critical slowing down (CSD). EWSs developed to capture CSD, such as autocorrelation⁴ and variance⁵ of the system variable are shown to increase prior to shifts in ecosystems⁹, climate system¹⁰, financial systems¹¹, lake food webs¹², and other dynamical systems. The applicability of CSD is limited to systems experiencing critical transitions that can be modeled using bifurcation theory⁷. However, the effectiveness of early warning signals (EWSs) in complex and diverse natural systems is often inconsistent^{4,13,14}. Even in systems that fit bifurcation models, obtaining reliable EWSs in real-world scenarios remains a significant challenge.

In real-world systems, where control parameters evolve over time, capturing and calculating EWS must be approached with caution. In cases of rapid environmental changes, significant external influences, or when system parameters shift too quickly for the system to stabilize, both the speed and reliability of EWS interpretation become crucial concerns¹⁵. Van der Bolt et al.¹⁶ have shown that the required data quantity depends on the range of system dynamics captured, rather than just the length of the dataset. Moreover, inherent fluctuations or noise in the system can trigger false alarms^{17,18}. To effectively use EWS in such practical systems, it is essential to quantify the reliability¹⁹ and sensitivity²⁰ of the signals for each specific system.

Even with a reliable EWS alert, implementing appropriate interventions needs sufficient warning time before tipping. It is not a trivial task to determine the minimum warning time required to mitigate the negative impact of the sudden shift^{21–23} and empirical evidence of successful reversal of regime shift using EWSs is rare²⁴. The minimum warning time depends on the response time to EWS detection, the ability to change the variables, and the speed of the system recovery after intervention²³ and all these aspects could vary according to the system.

Pavithran and Sujith²⁵ found that the rate at which the parameters vary affects both the available warning time and the tipping point. Parameters in natural and engineering systems evolve continuously. A finite rate of change of the bifurcation parameter results in rate-dependent tipping-delay^{25–27}; i.e., tipping occurs after crossing the bifurcation point (μ_0) in the case of bifurcation induced tipping (Fig. 1a,b). We notice that early warning for tipping is also delayed from the bifurcation point for fast variation of parameters. Receiving a warning after μ_0

¹Department of Aerospace Engineering, Indian Institute of Technology Madras, Chennai 600036, India. ²Centre of Excellence for studying Critical Transitions in Complex Systems, Indian Institute of Technology Madras, Chennai 600036, India. ³Data Science Department, National Physical Laboratory, Hampton Road, Teddington TW11 0LW, UK. ⁴Potsdam Institute for Climate Impact Research (PIK), 14473 Potsdam, Germany. ⁵Institute of Physics, Humboldt Universität zu Berlin, 12489 Berlin, Germany. ⁶Present address: The Jacob Blaustein Institutes for Desert Research, Ben Gurion University of the Negev, Beersheba, Israel. ✉email: juergen.kurths@pik-potsdam.de; sujith@iitm.ac.in

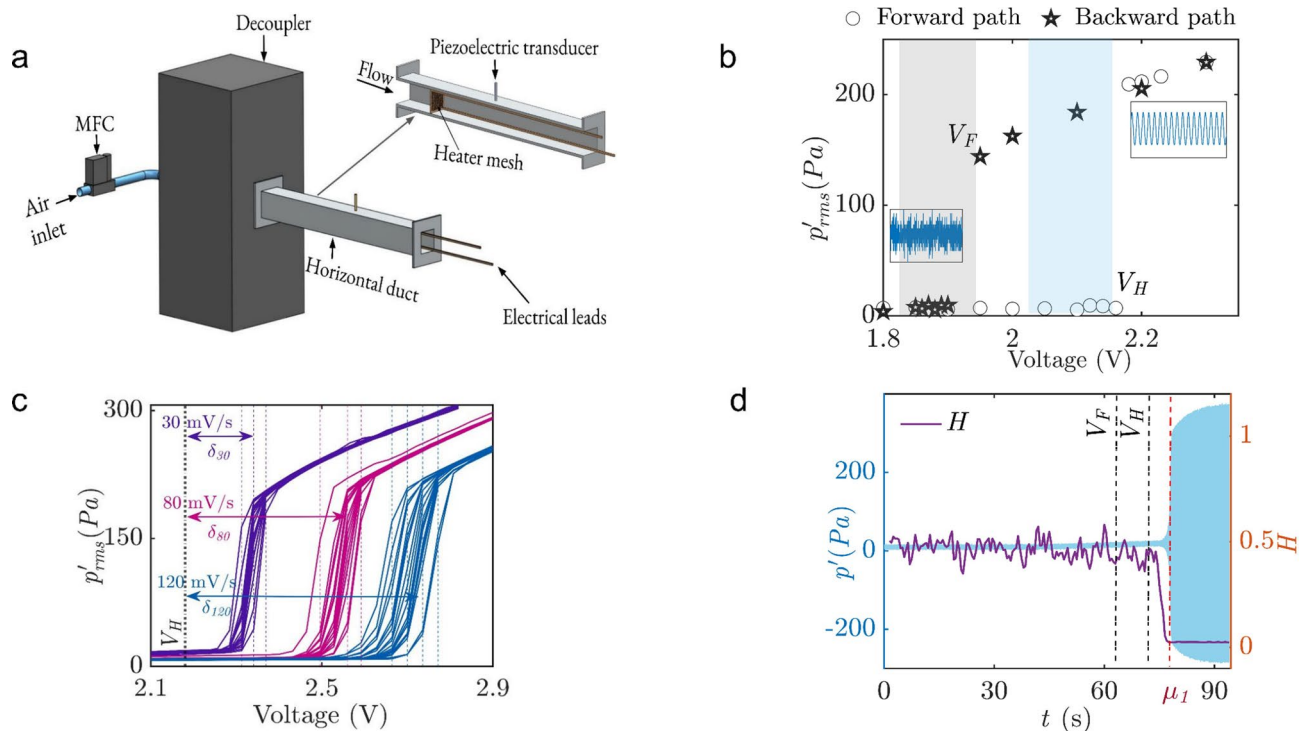


Fig. 2. System behavior in response to changes in control parameter (voltage supplied to the heater). **(a)** Schematic of the horizontal Rijke tube comprising a duct, an electrically heated wire mesh, and a decoupler, with a natural frequency of 162 Hz. **(b)** Variation of root mean square of acoustic pressure fluctuations (p'_{rms}) for a quasi-static experiment. \circ represents the forward path, with an abrupt jump of p'_{rms} at the Hopf point V_H (2.18 V), while \star represents the backward path, with a sudden drop to a safe operation state at the fold point V_F (1.95 V). Such a sudden shift from a safe operation state to TAI, i.e., fixed point to limit cycle (shown in inset) is a manifestation of Andronov Hopf bifurcation^{36–38}. Shaded regions represent V_H and V_F variations for 15 experimental realizations. **(c)** For continuous variation of voltage, tipping points are estimated by finding the maxima of dp'_{rms}/dt . The standard deviation in the tipping points is quantified using 20 realizations of experiments for 3 different rates (r). The onset of tipping (μ_1) is delayed by δ from V_H . As shown for rates 30 mV/s, 80 mV/s, and 120 mV/s, δ increases with an increase in the rate of change of voltage²⁵. **(d)** The variation in the value of H , along with the time series of acoustic pressure fluctuations as we vary the parameter linearly in time. The value of H decreases, providing an early warning of an impending tipping well before μ_1 .

(Fig. 4c,d). Out of 100 trials, prevention action was successful only in six trials. In the remaining 94 trials, the EWS alert is received at voltage values (between 2.54 V and 2.66 V) that are delayed compared to successful cases (between 2.46 V and 2.5 V), while the control parameter was varying rapidly. As a result, even a slight delay in the response of the device, relative to the timescale of the growth of amplitude, is sufficient for oscillations to grow. Consequently, the system transitions into periodic oscillations before the prevention action is complete. In spite of the borrowed window of safe operation provided by the delay in tipping due to rate, with increase in r , the EWS alerts are also received after crossing the Hopf point. As a consequence, even extreme prevention strategies, such as directly reducing the control parameter to a lower value within the bistable region, may be rendered ineffective.

When the prevention action for faster rates (Fig. 4c,d) falls short, we need to adopt an alternate approach. Abruptly lowering the control parameter below the fold point of the system (Fig. 4e,f) effectively controls the system after tipping; we refer to this action as control action (see “Methods”). The control action returns the system to the safe operating state (increase in H from 0 to 0.4–0.6 in Fig. 4f). For fast variation of parameter, where extreme prevention action fails, the control action emerges as the sole viable action for restoring the system to the state of safe operation. The control action can be useful in real-world systems that can tolerate oscillations for a short period.

Discussion

In this work, we have investigated the feasibility of real-time EWS-based prevention action in a real-world system - an experimental thermoacoustic system. Our findings provide a framework for utilizing EWS in practice for mitigating tipping in systems where sudden transitions pose significant operational risks. We systematically analyzed the relationship between the rate of change of a control parameter and the delay in the onset of tipping. We demonstrate that the delay in the onset of tipping in parameter increases with increasing the rate of change of parameter (Fig. 2c). Pace et al.²⁴ showed that by stopping the nutrient inputs in response to early warnings,

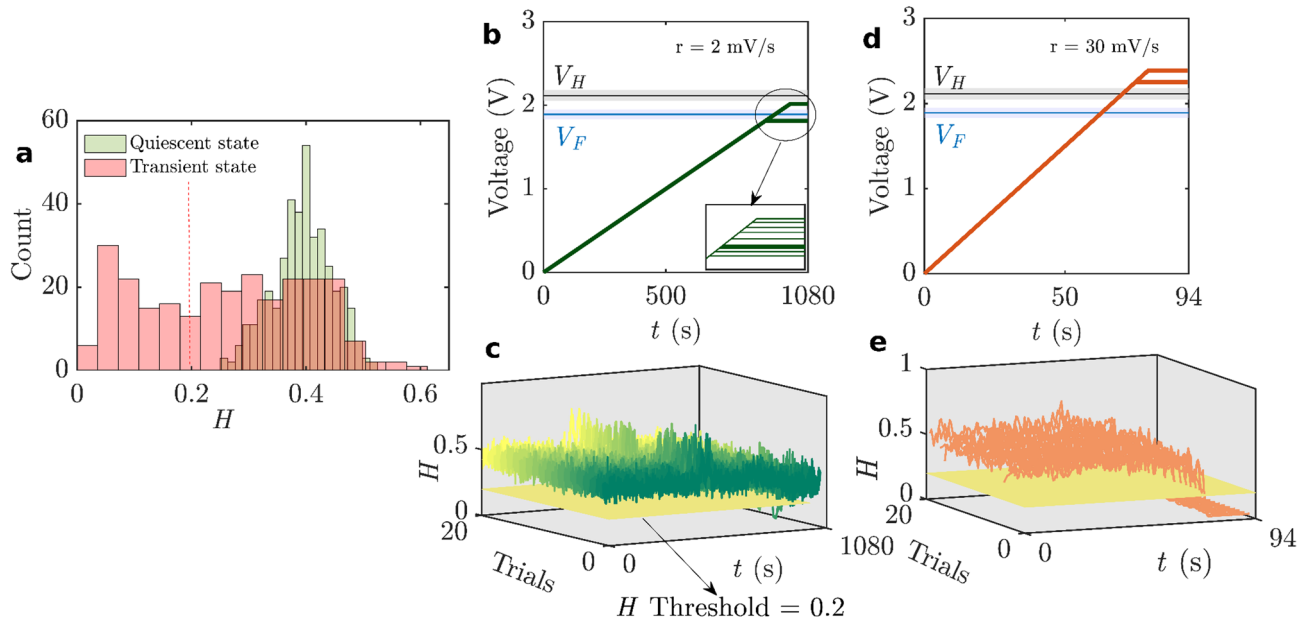


Fig. 3. Experimental demonstration of freeze action for a slow variation of parameter and failure of this prevention action under fast variation of parameter. **(a)** Distribution of values of H from multiple trials for the safe operation state (at 1.84 V; green) and the transient state (from 1.84 V till the onset of tipping; red) indicates that a value of 0.2 for H can distinguish these two states. **(b)** The voltage value at which we received EWS alert has variations. The voltage variation for 20 trials at $r = 2$ mV/s is shown in the inset, out of which the cases where we received the maximum and minimum values for EWS alerts shown in thick solid lines. **(c)** Upon receiving an EWS alert, the “freeze action” proves to be an effective prevention action, as we observe that the value of H rises to higher values after the prevention action (green shades depict different trials). **(d)** For $r = 30$ mV/s, we observe that the maximum and minimum values for EWS alerts are received above V_H . **(e)** For the case of fast variation of parameter $r = 30$ mV/s, the freeze action is not a viable solution, as observed from the value of H approaching zero (orange shades show different trials) indicating the presence of periodic content in the signal even after prevention action.

a quick recovery is possible as shown by the reversal of the manipulated lake to its original trophic state. We show that for a slow variation of parameter, rather than completely reducing the parameter value to zero, we stop the increase of the control parameter when we receive the early warning. Freezing the parameter at the point of receiving the EWS (referred to as the freeze action in this study) is an effective prevention action for slow variation of parameter. The freeze action is applicable in various systems, such as in thermofluid systems, pausing changes in the fuel supply can help suppress instabilities⁴⁰. In climate policy, halting the rate of deforestation at its current level can allow forest regeneration, particularly in tropical uplands⁴¹. Similarly, in economic systems, temporarily holding interest rates steady is often used as a short-term strategy to manage inflation expectations and stabilize the financial environment⁴². Such interventions help the system recover and stabilize without introducing further disturbances. In some systems, abruptly stopping the control parameter may push the system into an undesirable state via mechanisms such as shock-induced tipping⁴³. Within the time of operation, restarting the parameter from zero can lead to significant wastage of resources and energy, especially in real-world systems such as land-based gas turbines, where shutdown and restart costs are high⁴⁴. Thus, for the slow rate of variation of parameters, the freeze action proves to be effective in preventing tipping.

We employed the freeze action for fast variation of parameters and demonstrate that there is no unique action that can effectively prevent tipping across all operating conditions. Although EWS is detected before the tipping point, we found that in cases of fast variation of parameter, the warnings are received only after the control parameter has crossed the Hopf point. The EWS alert received after crossing the V_H is attributed to memory effects in the system^{45,46}. When the parameter changes at a finite rate, the system remains in the vicinity of the safe operating regime for some time, even after crossing the V_H . Additionally, the growth of oscillations requires a finite time to grow, during which the system parameter continues to evolve. As early warning indicators such as the H are computed from the time series data acquired from the system, this inherent delay is captured in the data and manifests as a corresponding delay in receiving the EWS alert. Even with the freeze action, the system is likely to drift into an undesirable state over time. This highlights the need for precise actions based on the specific operation conditions of the system. An obvious choice for prevention would be to reduce the control parameter to lower values^{21,26}. This action of reducing the control parameter, comes with a question, to what value the parameter should be reduced? This is a critical consideration, as reducing the parameter too much can significantly compromise the performance of the system. To address this question, for the system in our study, we further investigated the cases for fast variation of parameters. Through rigorous multiple trials, we showed that abruptly reducing the control parameter to a value within the bistable region proves to be an effective action

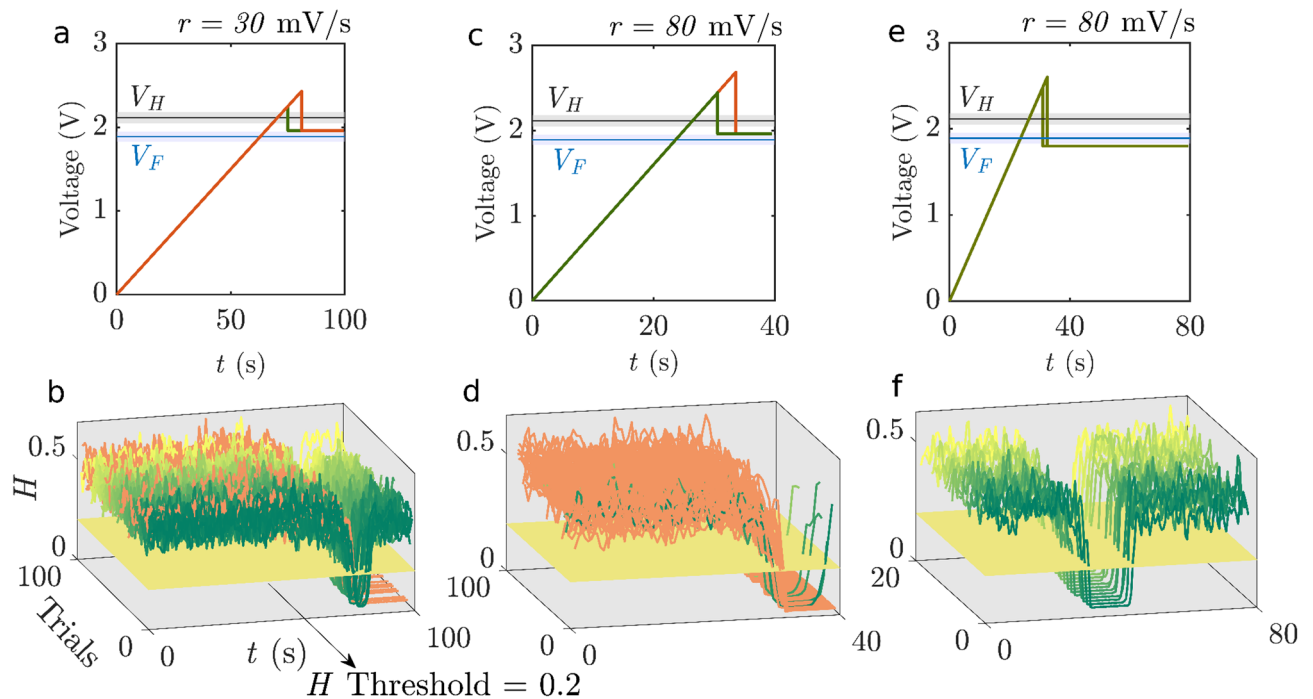


Fig. 4. EWS-based prevention action of direct cut-off to a lower value of control parameter within the bistable region for fast variation of parameter and alternative solution of control action. (a,c,e) The rate of variation of voltage illustrated for cases with lowest and highest EWS alert value for $r = 30$ mV/s, 80 mV/s and 120 mV/s is depicted. (b) For $r = 30$ mV/s, out of 100 realizations performed, the action of direct cut-off of voltage to a value of 1.96 V which lies within the bistable region successfully prevents tipping in 76% of trials (gradients of green color indicates these trials), while in the remaining 24% (gradients of orange color indicates these trials) EWS alerts are received farther away from Hopf point (V_H), resulting in tipping to TAI even after prevention action. (d) For $r = 80$ mV/s, we observe that EWS alerts are received at higher values of voltage compared to the $r = 30$ mV/s case. We could prevent the transition only in 6 realizations, with the prevention action of direct cut-off of voltage to 1.96 V. (f) In the case of $r = 80$ mV/s, where prevention action proves ineffective, lowering the control parameter to a value below the fold point allows us to bring back the system to its safe operational state. The system exhibits periodic oscillations for a finite duration before reverting to its safe operational state.

in preventing tipping for moderately fast rates. The concept of abruptly reducing a control parameter finds relevance in various domains. For example, predictive suspension of insulin delivery is employed to prevent patients from entering hypoglycemic states⁴⁷. Similarly, during an emergency sharp reduction in fuel flow rate is implemented in land-based gas turbine units⁴⁸ to avert potentially catastrophic outcomes. We show that such practical systems have a dependence on the perturbations in the system, and these can lead to variabilities in the stability boundaries, the onset of tipping points, and EWS-alert timings. Therefore, considering these variabilities is also crucial while performing real-time prevention actions in real-world systems.

We showed that the prevention action of abruptly reducing the control parameter to a value within the bistable region is not effective in preventing tipping if your rate of variation of the parameter is too fast ($r = 80$ mV/s, for this experimental system). For such fast variation of control parameter, EWS-alerts are received far from the Hopf point, rendering the prevention action less effective due to limited time for intervention. We demonstrate that in such cases where the prevention action fails, control actions (reducing to a control parameter value below the fold point) can be employed. The system experiences periodic oscillations temporarily for a certain period after which the system settles to the safe operation state. The experimental setup used in this study offers high-precision control over the control parameter, specifically the voltage supplied to the mesh. Moreover, the system is relatively simple and well-isolated from external influences such as complex flow dynamics or interactions with reactive processes, which are common in real-world thermo-fluid systems. This controlled environment is ideal for investigating fundamental features of tipping behavior. However may not capture the full spectrum of complexities present in natural or engineering systems. A further limitation lies in our reliance on time series data from a single sensor. While this has been effective for our current analysis, it does introduce vulnerability; sensor failure or noise could significantly affect the detection of early warning signals. In terms of generalizability, actions such as freezing or abruptly reducing the control parameter used here to prevent or control tipping may not be feasible in more complex or large-scale systems. These systems may exhibit richer dynamical behavior, including multiple intermediate states or competing instabilities, which are not captured in our simplified setup. Therefore, caution must be exercised when extrapolating our findings to more intricate real-world scenarios.

Studies show that CSD-based indicators are not always reliable^{16,19,49–54}. In part, this can be attributed to the fact that the assumed mechanism behind critical slowing down (bifurcation-induced tipping) may be too simplistic for many natural systems which call for data-driven indicators of resilience related to other transition scenarios^{55–57}. Focusing on developing more general resilience-based EWSs is also considered as one possible solution⁵⁸. We leave the choice of EWS to the practitioners since different EWSs work well for different systems. Even with all the different ways of getting EWS, there is a need to implement different actions to prevent the system from tipping.

The current study on a prototypical thermoacoustic system serves as the first experimental study exploring the reliability and limits of applicability of EWS in preventing tipping in real-time for a practical system. Recent studies have highlighted the potential of machine learning (ML) models⁵⁹ especially deep learning^{60,61} trained on synthetic or theoretical data, in detecting early warning signals associated with tipping points in complex systems. Experimental data especially from such well-controlled practical systems, provide a valuable opportunity, offering time series data generated under well-controlled conditions, with measurable uncertainties and clearly defined thresholds. Incorporating such data into the training and validation of ML-based early warning systems grounds these models in physical reality. This combined approach, integrating theoretical modeling with empirical validation, marks a significant advancement in developing robust and reliable early warning systems for both natural and engineering systems.

Methods

Quasi-static experiments

We perform experiments in a prototypical thermoacoustic system known as a horizontal Rijke tube (Fig. 2a). A horizontal Rijke tube is a 1 m long duct of cross-sectional area $0.093 \times 0.093 \text{ m}^2$. An airflow of 100 SLPM (2.04 g/s) is maintained throughout the experiments. The duct has two ends: one end is open to the atmosphere, and the other is connected to a decoupler, which is a large rectangular chamber. The decoupler (1.2 m \times 0.45 m \times 0.45 m) removes the inherent fluctuations in the incoming air before the air enters the Rijke tube. A wire mesh located 25 cm from the decoupler end is electrically heated, which acts as a compact source of heat in the Rijke tube. A piezoelectric pressure transducer (PCB103B02, sensitivity: 247.5 mV/kPa, resolution: 0.2 Pa, and uncertainty: 0.15 Pa) is mounted on the duct at a location 57 cm (i.e. near the pressure antinode of the fundamental duct mode) from the decoupler end to measure the acoustic pressure fluctuations in the system. We acquired the acoustic pressure fluctuations signal for each value of the control parameter for 6 s at a sampling frequency of 10 kHz (see Fig. 2b). A bin size of 0.17 Hz is used for obtaining the fast Fourier transform (FFT) of the acoustic pressure fluctuations time series. The fundamental frequency of the system is nearly 162 Hz. Prior to the experiments, under cold flow conditions, a sinusoidal signal is input to the Rijke tube using a loudspeaker, and then the loudspeaker is switched off abruptly. The acoustic pressure fluctuation decays when the loudspeaker is switched off, and by performing the Hilbert transform and calculating the logarithmic decay of acoustic pressure fluctuations data acquired, we determine the decay rate. A decay rate of $13 \pm 0.5 \text{ s}^{-1}$ is maintained for all the experiments conducted, to ensure that the experiments can be repeated.

When we increase the control parameter (referred to as the forward path in Fig. 2b), we observe the root mean square (RMS) value of the acoustic pressure fluctuations (p'_{rms}) is close to zero until a certain range of voltage values. As we increase the voltage, the system changes from a dynamical state known as fixed point (quiescent operation) to a state of limit cycle oscillations (high amplitude periodic oscillations) at a particular value of the control parameter. We observe a sudden rise in p'_{rms} , a characteristic of subcritical Hopf bifurcation^{36,38} and the voltage value corresponding to this sudden transition is considered as the value at the Hopf point (V_H). Subsequently, as we decrease the voltage (reverse direction), limit cycle oscillations display a steady decrease in amplitude. However, when we reverse the direction of control parameter, the transition from limit cycle to a fixed point occurs at the voltage value corresponding to the fold point (V_F), which is less than the V_H . We observe a hysteresis region, which is a characteristic of subcritical Hopf bifurcation. The horizontal Rijke tube with an electrically heated wire mesh, used in the present study, is a well-established experimental system for investigating thermoacoustic instability^{36,62,63}. For the current configuration, with the heating mesh placed at one-quarter the length of the tube, and using the input voltage supplied to the heater mesh as the control parameter, the system exhibits two distinguishable dynamical regimes: (1) A safe operational state, characterized by low-amplitude, aperiodic fluctuations, and (2) A state of thermoacoustic instability, marked by self-sustained, high-amplitude periodic oscillations. The representative time series corresponding to these two states is presented in Fig. 2b. No intermediate or transitional regimes are observed within the current experimental conditions and setup.

Selection of threshold for the Hurst exponent

In the current study, with the acquired acoustic pressure fluctuations signal, we compute the Hurst exponent (H) using the multifractal detrended fluctuation analysis⁶⁴ (MFDFA). In MFDFA, the value of H is calculated from the scaling of the root mean square (RMS) of the standard deviation of acoustic pressure fluctuations in relation to the data segment length. For the experiments with a finite rate of change of parameter, we compute the Hurst exponent with a window of 0.4 s data, overlapped by 0.2 s data. Our choice of window size is deliberate, as it strikes a balance between the efficient computation of H and the ability to issue timely warnings with only 0.2 s of data, affording more time for prevention action.

To determine the threshold for H , we acquired the acoustic pressure fluctuations for a quiescent operation state (below the fold point at 1.84 V) and corresponding values of H are depicted in (Fig. 3a in main text) as a histogram. To ascertain the transition state, we conducted multiple realizations, allowing the system to evolve from a quiescent state to a state of periodic oscillation. We then selected the values of H for the pressure fluctuations within the control parameter range from 1.84 V to the onset of tipping.

We aim to identify an optimal threshold that minimizes false alarms while providing sufficient time for prevention actions. Depending on the risk tolerance and specific requirements of the operator, the threshold can be tailored to initiate the necessary prevention strategy.

When the value of H crosses the threshold selected, we provide an EWS alert to initiate the prevention action. For a rate of change of parameter of 30 mV/s, the EWS alerts received for 20 trials each with different thresholds are depicted in Fig. 5. We observe that for a threshold of 0.3, the EWS alerts are received at very low voltage values compared to the voltage value at the onset of tipping (μ_1), giving false warnings (as shown in Fig. 5, blue circles). When we set the threshold to 0.2, as well as the threshold to 0.1, we find that the voltage corresponding to the EWS alert is close to μ_1 . However, the earlier the warning is received, the earlier we can perform the required prevention actions, to prevent the system from tipping. Hence, an EWS threshold of 0.2 is selected for initiating the prevention actions.

Receiver operating characteristics (ROC)

To assess the effectiveness of early warning signals (EWS), we employ the Receiver Operating Characteristic (ROC) curve, which captures the balance between the reliability (low false alarm rate) and sensitivity (ability to detect subtle changes) of an indicator. Following Boettiger and Hastings¹⁹ we construct the ROC by computing the true positive rate (TPR) and false positive rate (FPR) for different rates of change of parameter. For the present study, ROC curves quantify the ability of H in distinguishing the quiescent operation state (considered positive) and the transition to thermoacoustic instability (negative). We determine the,

True positive (TP) = cases rightly classified as positive.

True negative (TN) = cases rightly classified as negative.

False positive (FP) = cases actually negative but classified as positive.

False negative (FN) = cases actually positive but classified as negative.

Then we calculate the false positive rate (FPR) = $FP/(FP + TN)$ and the true positive rate (TPR) = $TP/(TP + FN)$. The FPR is plotted against the TPR for different threshold values for 3 different rates of change of parameter (shown in Fig. 6). For all the 3 cases, the curves remaining close to the top-left corner indicate that the classifier performs well^{15,65}. We also compute the area under the ROC curve (AUC) and observe values close to one indicating perfect distinction performed by the classifier.

Intervention strategies: prevention and control actions

We perform the following intervention strategies upon receiving an EWS alert:

- (1) Prevention strategy: For fast variation of control parameters, tipping occurs past the bifurcation point. EWS warns of an impending tipping within this tipping delay. However, the system will exhibit tipping if we stop varying the control parameter after receiving the alert, as we already crossed the bifurcation point by the time we get the EWS alert. Therefore, we immediately reverse the direction of variation of the control parameter; we lower the voltage to 1.96 V. We prevent the system from going to TAI by bringing the control parameter below the Hopf point (Refer Fig. 4a,b in main text).
- (2) Control strategy: When an EWS alert is obtained near the tipping point under fast variations, we have less warning time than slow parameter variations. In such scenarios, the system undergoes tipping while we reverse the control parameter. Here, reducing the voltage to a value lower than the Hopf point is not enough to prevent the system from tipping to TAI. Therefore, we reduce the control parameter below the fold point

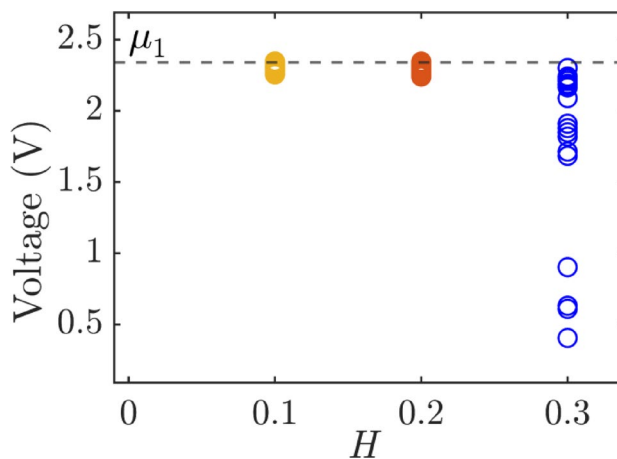


Fig. 5. Variation in the EWS alerts received for different thresholds. For a rate of 30 mV/s, the voltage at which the Hurst exponent crosses the threshold is plotted against the corresponding threshold for 20 realizations of experiment each with different thresholds. For a threshold of 0.3, alerts are received before the tipping point (μ_1). However, the variation across different trials is very high and includes many false warnings. For thresholds of 0.2 and 0.1, the alerts are received closer to μ_1 . A threshold value of 0.2 for H is found to be an optimum value with minimum false alarms and maximum warning time.

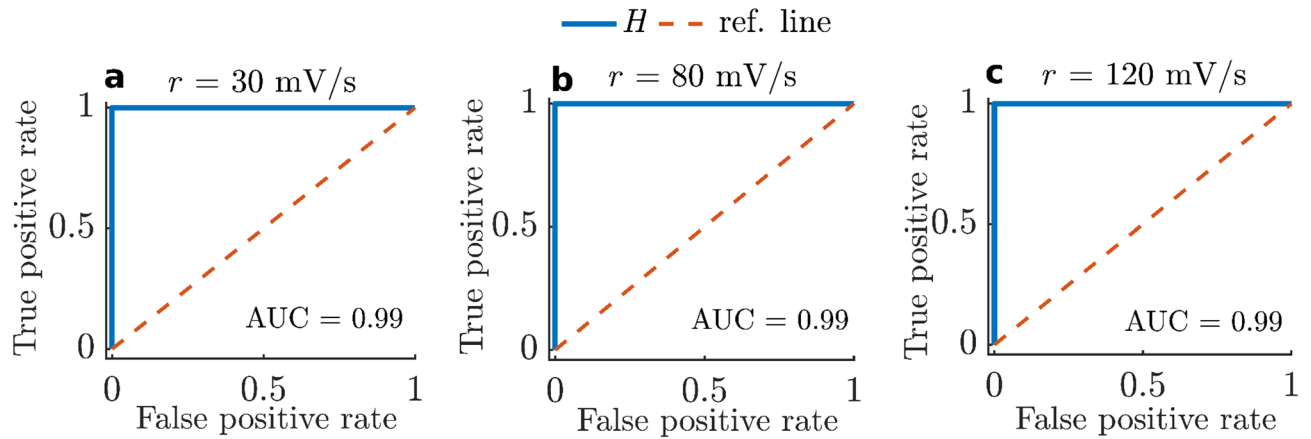


Fig. 6. ROC curves plotted using the values of H observed for rate of change of parameter (a) 30 mV/s (b) 80 mV/s (c) 120 mV/s. The area under the curve is nearly 0.99 for all cases indicating a perfect distinction performed by the classifier, compared to a random classification (depicted with dotted lines).

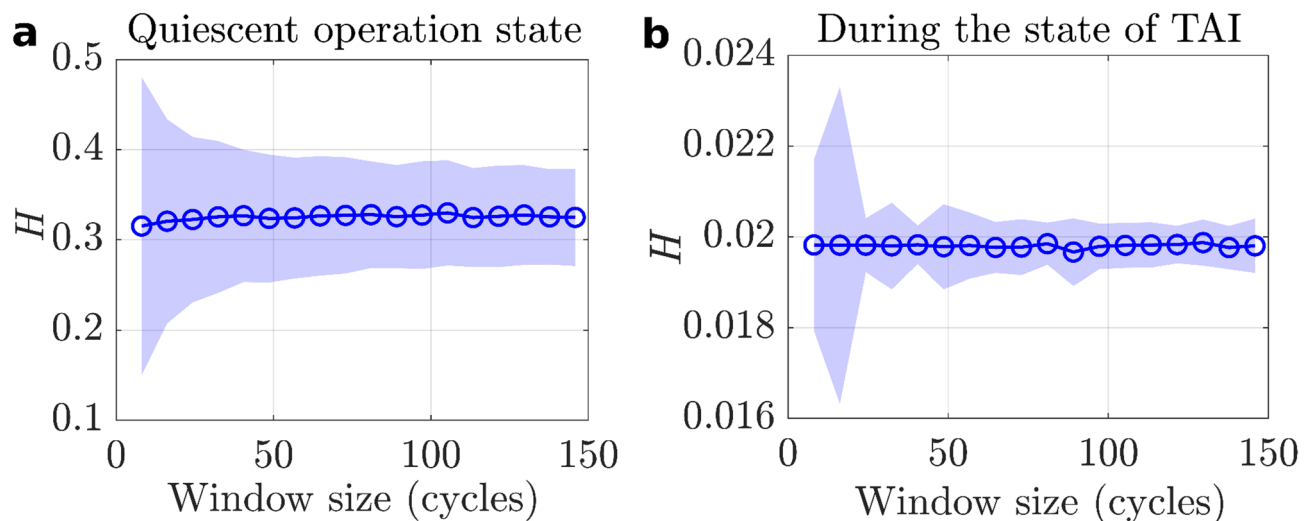


Fig. 7. Variations in the value of H for different moving window sizes at different states of operation in Rijke tube. The Hurst exponent with standard deviation corresponding to the quasi-steady time series of acoustic pressure fluctuations acquired at a sampling frequency of 10 kHz for a duration of 6 s with the size of the moving window for the states of (a) quiescent operation (b) during the state of TAI is plotted for 14 quasi-static experiments. For the window size of 50 acoustic cycles and above the value of H tends to a fixed value with small variance. In the current study, we used a window size of 64 cycles.

so that the system returns to the quiescent state immediately after the tipping. Thus, we call this a control strategy for mitigating TAI. We utilize such a technique in scenarios where the prevention strategy fails (Refer Fig. 4e,f in main text).

Quantification of the abrupt prevention actions

We define the window size for calculating the H , such that the value of H converges to a fixed value at different states of the system. We acquired the time series of acoustic pressure fluctuations at each state of the system under quasi-steady experiments. The data was acquired at a sampling frequency of 10 kHz for a period of 6 s. Figure 7 indicates that values of H converge to a fixed value for window size of 50 cycles and above. We selected 64 acoustic cycles as the window size for calculating H . For the experiments with a finite rate of change of parameter, we use a moving window of 0.4 s data with an overlap of 0.2 s data. The total time for calculating the H , comparing the value of H with the threshold and sending the signal to the DC power supply takes time of the order 10^{-4} s (clock time in Matlab).

Once the value of H crosses the threshold value of 0.2, we perform the prevention action of direct cut-off to a voltage value of 1.96 V. A programmable DC power supply (TDK - Lambda GEN 8-400 A) is used to control the voltage supplied to the heater mesh. The DC power supply has a response time of 20 ms; i.e., for a given input

value of voltage, it takes 20 ms for the DC power supply to reach the aforementioned voltage. Hence, reducing the voltage directly to a voltage value (either to a value within the bistable region or below the fold point) within 20 ms is an abrupt prevention or control action compared to the 0.2 s needed to acquire the next set of data. Since the response time is nearly one order higher than the time required for collecting the data, the prevention action of direct cut-off could be considered as the extreme case of prevention action.

Data availability

The data used in this study are available from the corresponding author upon reasonable request.

Received: 10 November 2024; Accepted: 9 June 2025

Published online: 23 June 2025

References

- Barabási, A. L. Network science. *Philos. Trans. Math. Phys. Eng. Sci.* **371**, 20120375 (1987).
- Scheffer, M. *Critical Transitions in Nature and Society* (Princeton University Press, 2009).
- Litt, B. et al. Epileptic seizures May begin hours in advance of clinical onset: a report of five patients. *Neuron*. **30** (1), 51–64 (2001).
- Dakos, V. et al. Slowing down as an early warning signal for abrupt climate change. *Proc. Natl. Acad. Sci. USA*. **105**, 14308–14312 (2008).
- Carpenter, S. R. & Brock, W. A. Rising variance: a leading indicator of ecological transition. *Ecol. Lett.* **9**, 311–318 (2006).
- Kosterlitz, J. M. The critical slowing down of relaxation processes near a second order transition. *J. Phys. C Solid State Phys.* **2** (11), 1787 (1969).
- Dakos, V., Carpenter, S. R., van Nes, E. H. & Scheffer, M. Resilience indicators: prospects and limitations for early warnings of regime shifts. *Philos. Trans. R. Soc. B.* **370**, 20130263 (2015).
- Kéfi, S., Dakos, V., Scheffer, M., Van Nes, E. H. & Rietkerk, M. Early warning signals also precede non-catastrophic transitions. *Oikos*. **122**, 641–648 (2013).
- Scheffer, M. et al. Early-warning signals for critical transitions. *Nature*. **461**, 53–59 (2009).
- Lenton, T. M. et al. Tipping elements in the earth's climate system. *Proc. Natl. Acad. Sci. USA*. **105**, 1786–1793 (2008).
- May, R. M., Levin, S. A. & Sugihara, G. Complex systems: ecology for bankers. *Nature* **451** (7181), 893 (2008).
- Carpenter, S. R. et al. Early warnings of regime shifts: a whole-ecosystem experiment. *Science* **332**, 1079–1082 (2011).
- Burthe, S. J. et al. Do early warning indicators consistently predict nonlinear change in long-term ecological data? *J. Appl. Ecol.* **53**, 666–676 (2016).
- Gsell, A. S. et al. Evaluating early-warning indicators of critical transitions in natural aquatic ecosystems. *Proc. Natl. Acad. Sci. USA*. **113**(50), E8089–E8095 (2016).
- Dai, L., Korolev, K. S. & Gore, J. Relation between stability and resilience determines the performance of early warning signals under different environmental drivers. *Proc. Natl. Acad. Sci. USA*. **112**(32), 10056–10061 (2015).
- van der Bolt, B. & van Nes Egbert, H. & Scheffer M. No warning for slow transitions. *J. R. Soc. Interface*. 1820200935 (2021).
- Livina, V. N., Ditlevsen, P. & Lenton, T. An independent test of methods of detecting system States and bifurcations in time-series data. *Phys. Stat. Mech. Appl.* **391**, 485–496 (2012).
- Perretti, C. T. & Munch, S. B. Regime shift indicators fail under noise levels commonly observed in ecological systems. *Ecol. Appl.* **22**, 1772–1779 (2012).
- Boettiger, C. & Hastings, A. Quantifying limits to detection of early warning for critical transitions. *J. R. Soc. Interface*. **9**, 2527–2539 (2012).
- Lenton, T. M., Livina, V. N., Dakos, V. & Van Nes, E. H. Early warning of climate tipping points from critical slowing down: comparing methods to improve robustness. *Philos. Trans. R. Soc. A.* **370**, 1185–1204 (2012).
- Biggs, R., Carpenter, S. R. & Brock, W. A. Turning back from the brink: detecting an impending regime shift in time to avert it. *Proc. Natl. Acad. Sci. USA*. **106**, 826–831 (2009).
- Carpenter, S. R., Brock, W. A., Cole, J. J. & Pace, M. L. A new approach for rapid detection of nearby thresholds in ecosystem time series. *Oikos* **123** (3), 290–297 (2014).
- Contamin, R. & Ellison, A. M. Indicators of regime shifts in ecological systems: what do we need to know and when do we need to know it? *Ecol. Appl.* **19** (3), 799–816 (2009).
- Pace, M. et al. Reversal of a cyanobacterial bloom in response to early warnings. *Proc. Natl. Acad. Sci. USA*. **114**(2), 352–357 (2016).
- Pavithran, I. & Sujith, R. I. Effect of rate of change of parameter on early warning signals for critical transitions. *Chaos: Interdiscip. J. Nonlinear Sci.* **31** (1), 013116 (2021).
- Ritchie, P. D. L., Clarke, J. J., Cox, P. M. & Huntingford, C. Overshooting tipping point thresholds in a changing climate. *Nature* **592**, 517–523 (2021).
- Scharpf, W. et al. Experimental observation of a delayed bifurcation at the threshold of an argon laser. *Opt. Commun.* **63**, 344–348 (1987).
- Ullon, W. & Forgoston, E. Controlling epidemic extinction using early warning signals. *Int. J. Dyn. Control*. **11**, 851–861 (2023).
- Suresh, S. *Fatigue of Materials* (Cambridge University Press, 1998).
- Culick, F. E. C. Unsteady motions in combustion chambers for propulsion systems. Tech. rep., AGARDograph, NATO/RTO-AG-AVT-039 (2006).
- Schob, W. Jr J. An experimental investigation of heat transfer and pressure effects on longitudinal combustion instability in a rocket motor using premixed gaseous propellants, Ph.D. thesis, Princeton University, USA (1963).
- Blomshield, F. S., Crump, J. E., Mathes, H. B., Stalnaker, R. A. & Beckstead M. W. Stability testing of full-scale tactical motors. *J. Propuls. Power*. **13** (3), 349–355 (1997).
- Gopalakrishnan, E. A., Sharma, Y., John, T. & Dutta, P. S. & Sujith R. I. Early warning signals for critical transitions in a thermoacoustic system. *Sci. Rep.* **6**, (2016).
- Livina, V. N. & Lenton, T. M. A modified method for detecting incipient bifurcations in a dynamical system. *Geophys. Res. Lett.* **34**, L03712 (2007).
- Hurst, H. E. Long-Term storage capacity of reservoirs. *Trans. Am. Soc. Civ. Eng.* **116**, 770–799 (1951).
- Matveev, K. California Institute of Technology. I. Thermoacoustic instabilities in the Rijke tube: Experiment modeling, Ph.D. thesis (2003).
- Balasubramanian, K. & Sujith, R. I. Thermoacoustic instability in a Rijke tube: Non-normality and nonlinearity. *Phys. Fluids*. **20**, 044103 (2008).
- Juniper, M. P. Triggering in the horizontal Rijke tube: Non-normality, transient growth and bypass transition. *J. Fluid Mech.* **667**, 272–308 (2011).
- Unni, V. R. et al. Interplay between random fluctuations and rate dependent phenomena at slow passage to limit-cycle oscillations in a bistable thermoacoustic system. *Chaos: Interdiscip. J. Nonlinear Sci.* **29**, 031102 (2019).

40. Rouwenhorst, D., Hermann, J. & Polifke, W. In situ identification strategy of thermoacoustic stability in annular combustors. *Int. J. Spray. Combust. Dyn.* **10** (4), 351–361 (2018).
41. Rudel, T. K., Defries, R., Asner, G. P. & Laurance, W. F. Changing drivers of deforestation and new opportunities for conservation. *Conserv. Biol.* **23** (6), 1396–1405 (2009).
42. Anari, A. & Kolari, J. W. Impacts of Monetary Policy Rates on Interest and Inflation Rates. Available at SSRN 3088133. (2017).
43. Feudel, U. Rate-induced tipping in ecosystems and climate: the role of unstable states, basin boundaries and transient dynamics. *Nonlin Processes Geophys.* **30**, 481–502 (2023).
44. O'Connor, J. & Noble, B. & Lieuwen T. Ground-based gas turbines. In *Renewable Fuels: Sources, Conversion, and Utilization* (Cambridge University Press, 2022).
45. Baer, S. M., Erneux, T. & Rinzel, J. The slow passage through a Hopf bifurcation: delay, memory effects, and resonance. *SIAM J. Appl. Math.* **49**, 55–71 (1989).
46. Bonciolini, G., Ebi, D., Boujo, E. & Noiray, N. Experiments and modelling of rate-dependent transition delay in a stochastic subcritical bifurcation. *R Soc. Open. Sci.* **5**, 172078 (2018).
47. Bruce, B. et al. Preventing hypoglycemia using predictive alarm algorithms and insulin pump suspension. *J. Diabetes Technol. Ther.* **11**, 93–97 (2009).
48. Teplov, B. E., Taradai, D. V. & Timin, A. V. Investigating the causes of the emergency shutdown of the gas turbine unit. *Power Technol. Eng.* **53**, 709–712 (2020).
49. Ditlevsen, P. D. & Johnsen, S. J. Tipping points: early warning and wishful thinking. *Geophys. Res. Lett.* **37**, L19703 (2010).
50. Clements, C. F., McCarthy, M. A. & Blanchard, J. L. Early warning signals of recovery in complex systems. *Nat. Commun.* **10**, 1681 (2019).
51. Diks, C., Hommes, C. & Wang, J. Critical slowing down as an early warning signal for financial crises?? *Empir. Econ.* **57**, 1201–1228 (2019).
52. Wilkat, T., Rings, T. & Lehnertz, K. No evidence for critical slowing down prior to human epileptic seizures. *Chaos: Interdiscip. J. Nonlinear Sci.* **29**, 091104 (2019).
53. Marconi, M. et al. Testing critical slowing down as a bifurcation Indicator in a Low- dissipation dynamical system. *Phys. Rev. Lett.* **125**, 134102 (2020).
54. Hagemann, A., Wilting, J., Samimizad, B. & Mormann, F. Priesemann V. Assessing criticality in pre-seizure single-neuron activity of human epileptic cortex. *PLoS Comput. Biol.* **17**, e1008773 (2021).
55. O'Keefe, P. E. & Wieczorek, S. Tipping phenomena and points of no return in ecosystems: beyond classical bifurcations. *SIAM J. Appl. Dyn. Syst.* **19**, 2371–2402 (2020).
56. Schoenmakers, S. & Feudel, U. A resilience concept based on system functioning: A dynamical systems perspective. *Chaos: Interdiscip. J. Nonlinear Sci.* **31**, 053126 (2021).
57. Kuehn, C., Zschaler, G. & Gross, T. Early warning signs for Saddle- escape transitions in complex networks. *Sci. Rep.* **5**, 13190 (2015).
58. O'Brien, D. A. et al. Early warning signals have limited applicability to empirical lake data. *Nat. Commun.* **14**, 7942 (2023).
59. Deb, S., Sidheekh, S., Clements, C. F., Krishnan, N. C. & Dutta, P. S. Machine learning methods trained on simple models can predict critical transitions in complex natural systems. *R. Soc. Open Sci.* **9**(2), 211475 (2022).
60. Bury T. M., Sujith R. I., Pavithran I., Scheffer M., Lenton T. M., Anand M., and Bauch C. T. Deep learning for early warning signals of tipping points. *Proc. Natl. Acad. Sci. USA.* **118**(39), e2106140118 (2021).
61. Huang, Y., Bathiany, S., Ashwin, P. & Boers, N. Deep learning for predicting rate-induced tipping. *Nat. Mach. Intell.* **6**, 1556–1565 (2024).
62. Gopalakrishnan, E. A. & Sujith, R. I. Influence of system parameters on the hysteresis characteristics of a horizontal Rijke tube. *Int. J. Spray. Combust. Dyn.* **6**, 293–316 (2014).
63. Mariappan, S., Sujith, R. I. & Schmid, P. J. Experimental investigation of non-normality of thermoacoustic interaction in an electrically heated Rijke tube. *Int. J. Spray. Combust. Dyn.* **7**, 315–352 (2015).
64. Ihlen, E. A. F. Introduction to multifractal detrended fluctuation analysis in matlab. *Front. Physiol.* **3**, 141 (2012).
65. Banerjee, A., Pavithran, I. & Sujith, R. I. Early warnings of tipping in a non-autonomous turbulent reactive flow system. efficacy, reliability, and warning times. *Chaos: Interdiscip. J. Nonlinear Sci.* **34**, 013113 (2024).

Acknowledgements

We thank Mr. Ambedkar S. and Mr. Dhadphale J. M for their help during the experiments. R.R. acknowledges the support from the Prime Minister Research Fellowship, Government of India. R.I.S. acknowledges the funding from IoE initiative (SP22231222CPETWOCTSHOC) and SERB/CRG/2020/003051 from the Department of Science and Technology, Government of India. We acknowledge the research support in part by the International Centre for Theoretical Sciences (ICTS) for the program “Tipping Points in Complex Systems” (code: ICTS/tipc2022/9). VNL was funded by the National Measurement System programme supported by the UK Government's Department for Science, Innovation and Technology.

Author contributions

R.R: Conceptualization (equal); data curation (lead); formal analysis (lead); investigation (lead); methodology (equal); validation (lead); visualization (lead); writing—original draft. I.P: Conceptualization (lead); formal analysis (equal); investigation (equal); methodology (equal); supervision (equal); writing—review & editing (equal). R. I. S: Conceptualization (equal); formal analysis (equal); funding acquisition (lead); investigation (equal); methodology (equal); project administration (lead); supervision (lead); writing—review & editing (equal). V. L: Supervision (equal); writing—review & editing (equal), investigation (supporting); methodology (supporting); J. K: Supervision (equal); writing – review & editing (equal), investigation (supporting); methodology (supporting). All authors reviewed the manuscript.

Declarations

Competing interests

The authors declare no competing interests.

Additional information

Correspondence and requests for materials should be addressed to J.K. or R.I.S.

Reprints and permissions information is available at www.nature.com/reprints.

Publisher's note Springer Nature remains neutral with regard to jurisdictional claims in published maps and institutional affiliations.

Open Access This article is licensed under a Creative Commons Attribution-NonCommercial-NoDerivatives 4.0 International License, which permits any non-commercial use, sharing, distribution and reproduction in any medium or format, as long as you give appropriate credit to the original author(s) and the source, provide a link to the Creative Commons licence, and indicate if you modified the licensed material. You do not have permission under this licence to share adapted material derived from this article or parts of it. The images or other third party material in this article are included in the article's Creative Commons licence, unless indicated otherwise in a credit line to the material. If material is not included in the article's Creative Commons licence and your intended use is not permitted by statutory regulation or exceeds the permitted use, you will need to obtain permission directly from the copyright holder. To view a copy of this licence, visit <http://creativecommons.org/licenses/by-nc-nd/4.0/>.

© The Author(s) 2025